



ARTICLE

Modified citrus pectin inhibits breast cancer development in mice by targeting tumor-associated macrophage survival and polarization in hypoxic microenvironment

Lei Wang¹, Lin Zhao¹, Fu-lian Gong¹, Chao Sun¹, Dan-dan Du¹, Xiao-xia Yang¹ and Xiu-li Guo¹

Large amounts of tumor-associated macrophages (TAM), which are predominately localized in hypoxia area of the tumor tissue, are associated with the malignant progression of the tumor. In the present study, we investigated the inhibitory effects of modified citrus pectin (MCP), a natural dietary polysaccharide, on the survival and polarization of TAM in relation to its inhibition on the growth and migration of breast cancer. M2 macrophages polarized from human monocyte THP-1 were chosen as a model for TAM. We showed that MCP (0.06%–1%) concentration-dependently suppressed the survival of TAM through inhibiting glucose uptake with a greater extent in hypoxia than in normoxia. Furthermore, MCP treatment decreased ROS level in TAM through its reducibility and inhibiting galectin-3 expression, leading to inhibition of glucose transporter-1 expression and glucose uptake. In addition, MCP suppressed M2-like polarization via inhibiting STAT3 phosphorylation. Moreover, the tumor-promoting effect of TAM could be restrained by MCP treatment as shown in human breast cancer MDA-MB-231 cells in vitro and in mouse breast cancer 4T1-luc orthotopic and metastasis models. In both tumor tissue and lung tissue of the mouse tumor models, the number of TAM was significantly decreased after MCP treatment. Taken together, MCP may be a promising agent for targeting TAM in tumor hypoxic microenvironment for breast cancer treatment.

Keywords: breast cancer; tumor-associated macrophages; tumor hypoxic microenvironment; M2-like polarization; modified citrus pectin; glucose transporter-1; galectin-3 inhibitor

Acta Pharmacologica Sinica (2022) 43:1556–1567; <https://doi.org/10.1038/s41401-021-00748-8>

INTRODUCTION

Large number of tumor-associated macrophages (TAM) which are predominately localized in hypoxia area of the tumor tissues, play an important role in tumor occurrence, growth, invasion, metastasis, angiogenesis, and lymphangiogenesis [1]. Thus, TAM have been reported to be an attractive target for tumor immunotherapy. Although some strategies have been found for tumor treatment based on TAM, they are reported to lack specificity or have serious side effects that hamper their application in the clinic [2]. Thus, it is still urgently needed to explore anti-TAM agents for the management of cancer.

Galectin-3, a β -galactoside-binding lectin, is involved in tumor proliferation, apoptosis, adhesion, metastasis, drug resistance, and immunosuppression. It has also been reported to play a significant role in many aspects of macrophage biology, such as migration, apoptosis, phagocytosis, and adhesion [3], indicating that galectin-3 might be a potential target for TAM to be involved in the tumor-promoting effects of TAM.

Recent years, a variety of galectin-3 inhibitors such as carbohydrates, peptides, antibodies, and nucleic acids have been developed to interfere in the binding of galectin-3 with endogenous ligands [4, 5]. Among them, modified citrus pectin (MCP), a pectin polysaccharide rich in galactose obtained by hydrolyzing citrus pectin with a small molecular weight, a low degree of esterification,

and no branching, is one of the most studied galectin-3 inhibitor [6]. Reports have shown that MCP could inhibit the proliferation or metastasis of prostate, breast, and colon cancer by inhibiting galectin-3 in tumor cells [7–9]. However, whether MCP could inhibit galectin-3 in TAM and prevent their tumor-promoting effects is remained unknown.

In the present study, we investigated the inhibitory effects and underlying mechanisms of MCP on the survival and polarization of TAM in tumor hypoxic microenvironment and found that MCP inhibited the growth and migration of breast cancer in vitro and in vivo.

MATERIALS AND METHODS

Reagents

PectaSol-C MCP (EcoNugenics, SantaRosa, USA); WZB117 (MCE, NJ, USA); NAC (Sigma, Hamburg, Germany); H₂O₂ (Sigma, Hamburg, Germany).

Cell lines

Human breast cancer cell line MDA-MB-231 (MM231), human monocyte THP-1 cells were purchased from cell bank of the Chinese Academy of Science (Shanghai, China). Human umbilical vein endothelial cells (HUVECs) was obtained from ATCC (Rockville,

¹Department of Pharmacology, Key Laboratory of Chemical Biology (Ministry of Education), School of Pharmaceutical Sciences, Shandong University, Ji-nan 250012, China
Correspondence: Xiu-li Guo (guoxl@sdu.edu.cn)

Received: 25 January 2021 Accepted: 20 July 2021

Published online: 30 August 2021

USA). Mouse breast cancer cell line 4T1 labeled with luciferase (4T1-luc) were kindly provided by Caliper (Hopkinton, USA).

Polarization of macrophage from THP-1

Polarization of macrophage was performed as previously described [10]. Polarization of resting macrophages (M0) of THP-1 was induced via a 24 h exposure to PMA (Sigma, Germany). Then M0 macrophages were polarized toward M1 or M2 phenotype by stimulation with LPS (Sigma, Germany) and TNF- α (PeproTech, USA) or with IL-4 /IL-13 (PeproTech, USA) for 72 h, respectively.

Isolation of murine bone marrow-derived macrophages (BMDM) BMDM were isolated following a standard protocol [11]. In brief, femur and tibia bones are collected from C57BL6/J mice and bone marrow cells were flushed out using red blood cell lysis buffer. Then BMDM cells are cultured in BMDM growth medium (RPMI-1640 supplemented with 10% FBS, 50 ng M-CSF) for 7 days.

Cell viability assay

Cell viability was measured according to cell counting kit-8 assay (CCK-8, DOJINDO, Japan) protocol by measuring the absorbance at 450 nm. THP-1 cells were plated into 96-well microtiter plates. After polarized into M2 phenotype, the cells were treated with serial concentrations of MCP (in PBS) for 24 h. 10% CCK-8 was added to each well and incubated for 3 h. The absorbance was measured at 450 nm using a microplate reader (Thermo Fisher Scientific, Inc.).

Western blotting analysis

Western blot was performed as previously described [10]. In brief, proteins were separated by 10% SDS-PAGE and transferred to PVDF membrane (Millipore, Billerica, USA). After blocking in 5% (w/v) skim milk overnight, membranes were probed with primary antibodies against human HIF-1 α (#36169), STAT3 (#12640) and p-STAT3 (#9145) (CST, USA), galectin-3 (#14979-1-AP), GLUT-1 (#21829-1-AP) and NRP-1 (#16396-1-AP) (Proteintech, China), and anti- β -actin (#ZF-0313, ZS Bio, China) overnight, and incubated with secondary antibodies goat anti-mouse or anti-rabbit IgG. Membranes were detected using a ChemiDoc XRS molecular imager (Bio-Rad, CA, USA).

Glucose uptake assay

Glucose concentration in medium supernatant of cells was detected according to the protocol of Glucose Assay Kit (NJJCBIO, Wuhan, China). The amount of glucose uptake is equal to the amount of glucose in fresh medium minus the amount of glucose in the medium supernatant of treatment group. Cells were collected and the number of cells was counted by cell counter. The values of glucose level were normalized to the number of cells.

Lactate acid assay

After polarized into M2 phenotype, the cells were treated with serial concentrations of MCP (in PBS) for 24 h. The lactate acid contents were determined using Lactic Acid kit (NJJCBIO, Wuhan, China) following the manufacturer's instructions. Cells were collected and the number of cells was counted by cell counter.

Quantitative real-time PCR (qRT-PCR)

qRT-PCR was performed as previously described [10]. In brief, RNA was extracted from macrophage by using TRIzol method (Invitrogen, California, USA). Total RNA was reversely transcribed into cDNA using a qPCR RT Kit (Toyobo, Osaka, Japan), according to the manufacturer's instructions. Target gene sequences were purchased from Ji-nan Boshang Biotechnology Co., Ltd, the primers sequences as below: GLUT-1 (5'-3'): CAGCCGATGTGACCC GAGAC; galectin-3 sequence (5'-3'): ATGCAAACAGAATTGCTTT AG; TGF- β sequence (5'-3'): GCAACAATTCCTGGCGATACC; VEGFA

sequence (5'-3'): GCAGAATCATCACGAAGTGGT; IL-10 sequence (5'-3'): TCTCCGAGATGCCTTCAGCAGA; IL-1R sequence (5'-3'): GAC ATTCTGCCGTTACAGTCCAG.

Antioxidant assay

The antioxidant capacity was measured with an Antioxidant Assay Kit (NJJCBIO, China) following the manufacturer's instructions. In the assay protocol, ABTS is oxidized to green ABTS⁺ under the action of appropriate oxidant, and the production of ABTS⁺ will be inhibited in the presence of antioxidants. The total antioxidant capacity of samples can be determined and calculated by measuring the absorbance of ABTS⁺ at 405 nm.

Cell transfection

Cell transfection was determined according to Micropoly-transfecter Cell Reagent (#MT115, Micropoly, Nantong, China) protocol. The sequence of galectin-3-siRNA was 5'-CAC GCT TCA ATG AGA ACA ACA-3'. The sequence of scrambled control was 5'-TTC TCC GAA CGT GCT GTC TTT-3'.

Preparation of conditioned medium (CM)

After polarization or treatment, the cells were cultured in serum-free medium for 48 h. The medium supernatant was collected, centrifuged (1000 \times g, 5 min) and filtered through a 0.22- μ m syringe filter, and stored at -80 $^{\circ}$ C until use.

In vitro angiogenesis or vascular mimicry assay

In vitro angiogenesis or vascular mimicry assay was performed as previously described [10]. In brief, MM231 cells or HUVECs were added into 96-well plate precoated with 100 μ L Matrigel and cultured with 100 μ L CM for 6 h at 37 $^{\circ}$ C. The total branching length of tube, which represent the tube forming ability of cells, was calculated by ImageJ software.

Transwell co-culture system

After treated with MCP, M2 macrophage was co-cultured with MM231 in transwell chamber (Corning, NY, USA) for 48 h. The MM231 cells on the bottom side of the transwell chamber were stained with crystal violet, and counted.

ELISA

After treatment with MCP, the cells were cultured in serum-free RPMI-1640 medium for 24 h. The supernatant of the culture medium was collected, centrifuged at 1000 \times g for 5 min, and stored at -20 $^{\circ}$ C. The levels of TGF- β and VEGFA in culture supernatants were assessed separately using ELISA kits (Proteintech, China) according to the manufacturer's instructions.

Flow cytometry

Surface marker expression in M2-polarized THP-1 was analyzed by flow cytometry. After polarization, macrophages were collected into a 1.5 mL tube and incubated with 3% BSA for 1 h. Then cells were stained with anti-human CD163-PE antibodies (333605; Biolegend, California, USA) or anti-human CD68-FITC antibodies (333805; Biolegend, California, USA) at 4 $^{\circ}$ C for 1 h. Upon labeling, cells were washed, suspended in PBS. Data acquisition was performed using the BD FACS Calibur cytometer (Becton Dickinson, CA, USA).

Tumor model and IVIS imaging

Balb/c mice (female, 5-week-old) were purchased from the Animal Center of China Academy of Medical Science (Beijing, China). All animal experiment protocols were conducted in strict accordance with the Institutional Guidelines of Animal Care and Use Committee of Shandong University.

4T1-luc orthotopic tumor mouse model: 4T1-luc cells (5×10^5 /100 μ L/each mouse) were injected into the mammary fat pad under #3 mammary gland of each mouse. When the tumor

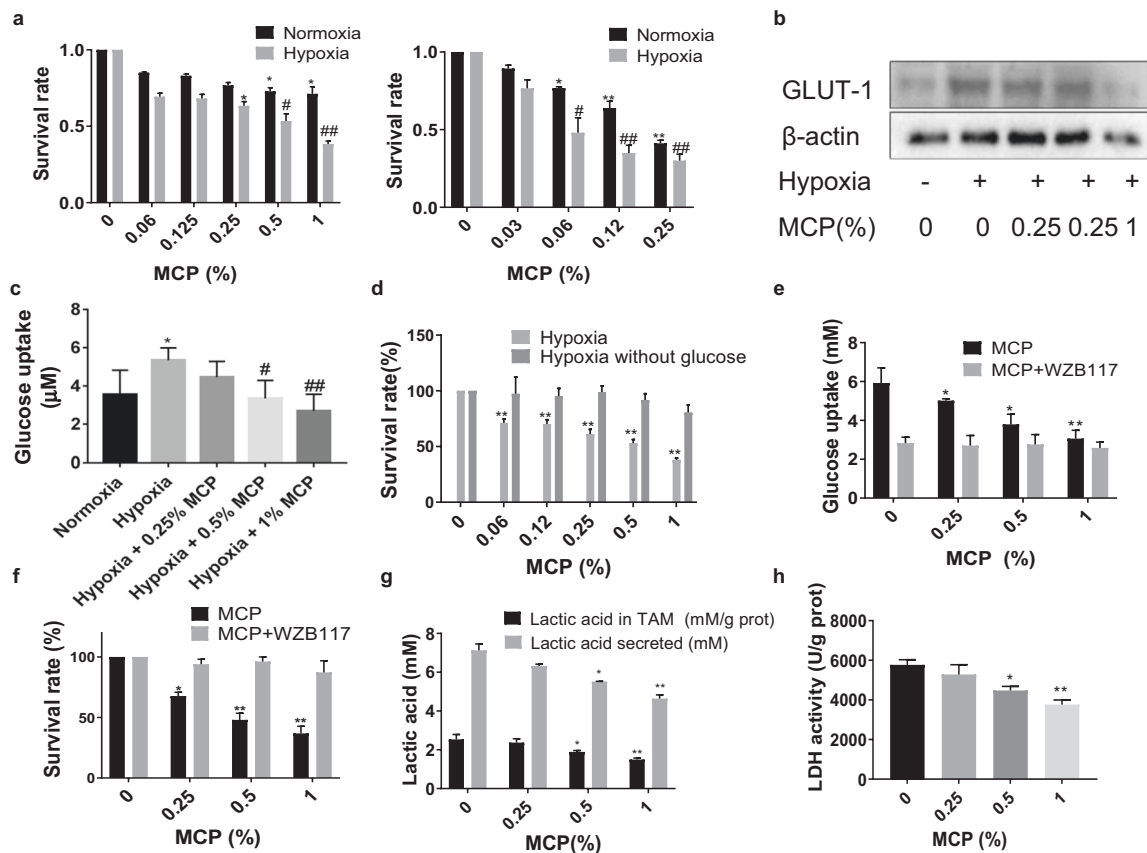


Fig. 1 MCP inhibited the survival of TAM in hypoxia by reducing glucose uptake via downregulation of GLUT-1. **a** TAM were treated with MCP at the indicated concentrations for 24 h. Oxygen deprivation (1% O₂) was achieved by culturing cells in hypoxic chambers. Effects of MCP on cell viability of TAM was detected by CCK-8 assay. Left: THP1-derived TAM; right: BMDM-derived TAM. **b** Effect of MCP on the expression of GLUT-1 in TAM at the indicated concentrations for 24 h was detected by Western blotting. **c** The glucose uptake of TAM treated with MCP in hypoxia was determined by glucose assay kit. **d** Effect of MCP on cell viability of TAM in glucose-free medium at the indicated concentrations for 24 h was detected by the CCK-8 assay. **e** The glucose uptake of TAM treated with MCP or/and WZB117 (10 μM) under hypoxia for 24 h was detected by the glucose assay kit. **f** Effect of MCP or/and WZB117 on cell viability of TAM in hypoxia at the indicated concentrations for 24 h was detected by the CCK-8 assay. **g** The lactic acid in medium supernatant of TAM and the content of lactic acid in TAM in hypoxia for 24 h were detected by lactic acid assay. **h** The LDH activity in TAM in hypoxia for 24 h was detected by LDH assay. All the experiments have been repeated three times. **P* < 0.05, ***P* < 0.01, vs. normoxia control group of; #*P* < 0.05, ##*P* < 0.01, vs. respective hypoxia control group.

volume reached about 100 mm³, MCP (low-dose: 350 mg/kg every day; high-dose: 700 mg/kg every day) was given orally at once a day, clodronate liposomes (100 μL/10 g) was administered intravenously every 3 days. Each treatment was performed for consecutive 28 days.

4T1-luc metastasis tumor mouse model: 1 × 10⁵ 4T1-luc cells (1 × 10⁵/100 μL/each mouse) were intravenously injected to each mouse by tail vein. MCP (low-dose: 350 mg/kg every day; high-dose: 700 mg/kg every day) was given orally at once a day, clodronate liposomes (100 μL/10 g) was administered intravenously every 3 days. Each treatment was performed for consecutive 21 days.

The 4T1-luc cells in mouse were monitored using the IVIS Kinetic in vivo imaging system (Caliper Life Sciences, MA, USA) at 9 min after D-luciferin potassium salt was injected intraperitoneally. At the end of experiments, the xenografts and lungs of mice were removed and weighed.

Immunohistochemical staining assay

Frozen cryosections for tumors or lung tissues of tumor model were fixed with acetone, and permeabilized with 0.2% Triton X-100. After blocked with 3% BSA, the section was immunostained with rabbit anti-CD31 (1:100; #3529, CST, Boston, MA), anti-mouse CD68-FITC (1:50, #137005, Biolegend, CST, Boston,

MA) and anti-mouse CD206-PE (1:50, #141706, Biolegend, CST, Boston, MA). Immunostainings were analyzed by using the fluorescence microscope (NIKON Ti-U, Nikon, Japan).

Statistical analysis

Data were expressed as mean ± SD and analyzed by Student's *t*-test. A *P*-value < 0.05 was considered statistically significant. Statistical analysis was performed using the Graphpad Prism 7.0 software.

RESULTS

MCP inhibited the survival of TAM in hypoxia by reducing glucose uptake via downregulation of GLUT-1 in vitro

We chose M2 macrophage polarized from THP-1 as a model for TAM. TAM was treated with different concentrations of MCP ranging from 0.06% to 1% (*w/v*) for 24 h and cell survival fraction was assessed by CCK-8 assay. The result showed that MCP inhibited the survival of two kinds of TAM derived from THP-1 in a concentration-dependent manner under normoxia and hypoxia (*P* < 0.05). And MCP showed a higher inhibitory effect in hypoxia than that in normoxia. Moreover, MCP had the same inhibitory effect on the survival of BMDM-derived TAM (Fig. 1a). Then we observed that MCP could reduce the expression of glucose

transporter-1 (GLUT-1) (Fig. 1b) and inhibit the glucose uptake in hypoxia TAM in a dose-dependent manner (Fig. 1c). Next, a glucose-free medium was used to culture TAM to further confirm the inhibitory effects of MCP on the survival of TAM depending on glucose uptake. The result showed that MCP had no significant inhibitory effect on the survival of TAM in glucose-free medium (Fig. 1d). These results suggested that MCP might decrease the survival of TAM by inhibiting glucose uptake.

Furthermore, WZB117, an inhibitor of GLUT-1, was introduced to confirm the role of GLUT-1 in the inhibitory effect of MCP. Compared with treatment with WZB117 alone, the combination of MCP at different concentrations and WZB117 did not enhance the inhibition of glucose uptake (Fig. 1e) and the survival of TAM in hypoxia obviously (Fig. 1f). This suggested that MCP could inhibit glucose uptake via downregulation of GLUT-1 expression, which in turn inhibited the survival of TAM, especially in the hypoxic microenvironment.

Besides, MCP also inhibited the content and release of lactic acid and activity of LDH in hypoxia TAM, indicating that MCP further inhibited the glycolysis of TAM (Fig. 1g, h).

MCP downregulated GLUT-1 expression of TAM by inhibiting galectin-3 and ROS
Reactive oxygen species (ROS) was reported to induce GLUT-1 expression in endothelial cells by increasing the accumulation of

hypoxia-inducible factor-1 α (HIF-1 α) [12]. So the effect of MCP on ROS level and the expression of redox-sensitive transcription factor Nrf-2 in TAM was detected. Results showed that MCP significantly reduced the level of ROS and the expression of Nrf-2 in hypoxic TAM (Fig. 2a, b), indicating that ROS might be involved in the downregulation of GLUT-1 expression induced by MCP. To verify this point, H₂O₂ was introduced to TAM treated with MCP. As shown in Fig. 2c, H₂O₂ reversed the inhibition of GLUT-1 expression by MCP under hypoxia, as well as the effect of MCP on TAM survival and glucose uptake (Fig. 2d, e). To determine whether the downregulation of GLUT-1 expression by MCP was related to the inhibition on HIF-1 α , the transcription factor of GLUT-1, we observed the effects of MCP and ROS on the transcriptional activity of HIF-1 α . Immunofluorescence result showed that either MCP or antioxidant N-acetyl-L-cysteine (NAC) inhibited the hypoxia-induced nuclear translocation of HIF-1 α (Fig. 2f), H₂O₂ reversed the inhibitory effect of MCP on HIF-1 α nuclear translocation (Fig. 2g), suggesting that MCP inhibited HIF-1 α nuclear translocation by reducing ROS level in TAM. Next, we introduced the HIF-1 α inhibitor 2ME2 to observe the effect of HIF-1 α on the GLUT-1 expression in hypoxic TAM. The result showed that MCP, NAC, or 2ME2 reduced the mRNA expression of GLUT-1 in TAM under hypoxia (Fig. 2h). After the introduction of 2ME2, the inhibitory effect of MCP on hypoxic TAM survival was reduced (Fig. 2i). Together, these results suggested that MCP

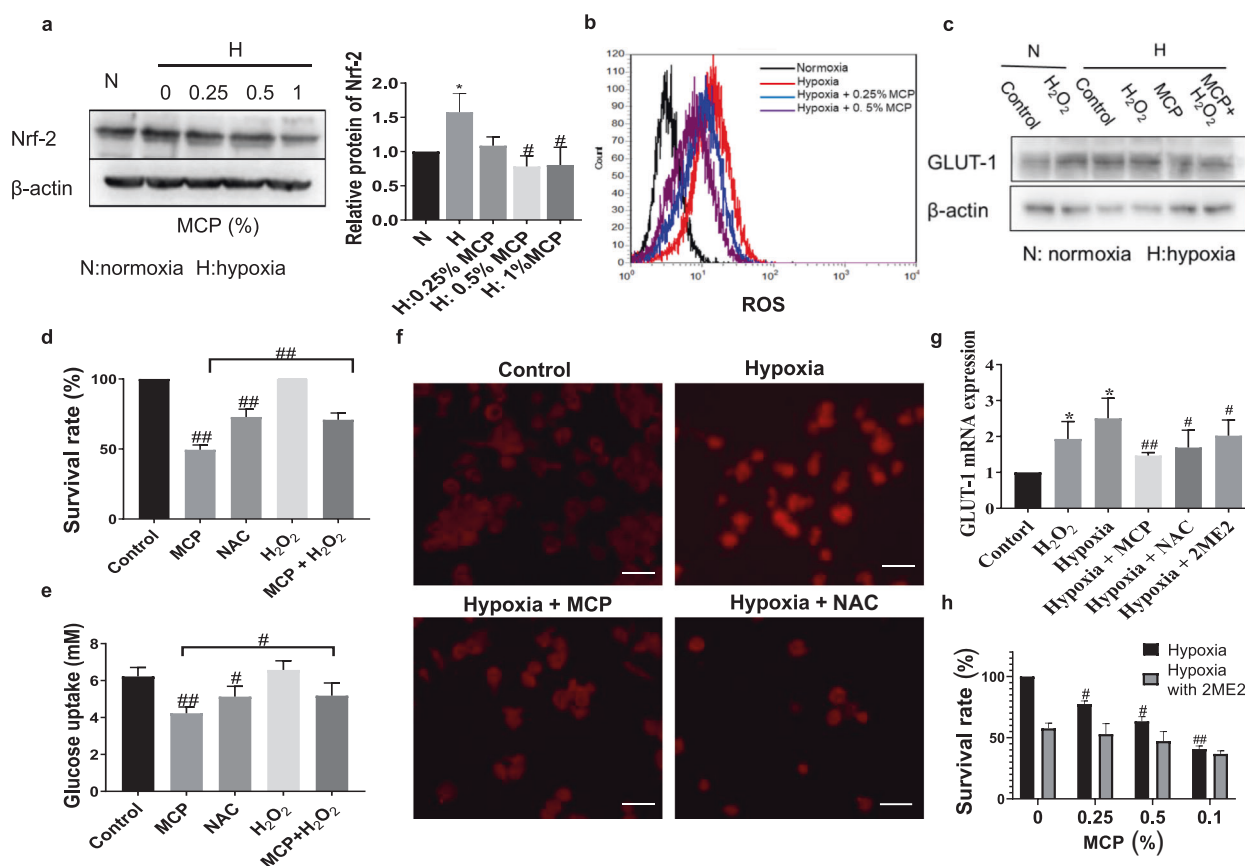


Fig. 2 MCP inhibited GLUT-1 expression of TAM by inhibiting ROS and HIF-1 α . **a** Effect of MCP on the expression of Nrf-2 in TAM at the indicated concentrations for 24 h was detected by Western blotting method. **b** Effect of MCP on the ROS level was detected by flow cytometry method. **c** Effect of H₂O₂ (10 μ mol/L) on the GLUT-1 expression of TAM in hypoxia treated with MCP for 24 h was detected by Western blotting method. **d** Effect of H₂O₂ on the survival of TAM treated with MCP in hypoxia for 24 h was detected by CCK-8 assay. **e** Effect of H₂O₂ on the glucose uptake of TAM treated with 0.5% MCP in hypoxia for 24 h was detected by the glucose assay kit. **f** Immunofluorescence images of HIF-1 α in hypoxia TAM treated with 0.5% MCP, NAC (10 nM, pretreatment for 1 h) (magnification, \times 100, bar = 200 μ m). **g** Effects of 0.5% MCP, NAC (10 nM, pretreatment for 1 h) and 2ME2 (10 μ M, pretreatment for 0.5 h) on mRNA expression of GLUT-1 in TAM under hypoxia were assessed by RT-PCR. **h** Effect of MCP or/and 2ME2 (10 μ M, pretreatment for 0.5 h) on cell viability of TAM in hypoxia at the indicated concentrations for 24 h was detected by the CCK-8 assay. All the experiments have been repeated three times. * P < 0.05 vs. respective normoxia control group, # P < 0.05, ## P < 0.01, vs. respective hypoxia control group.

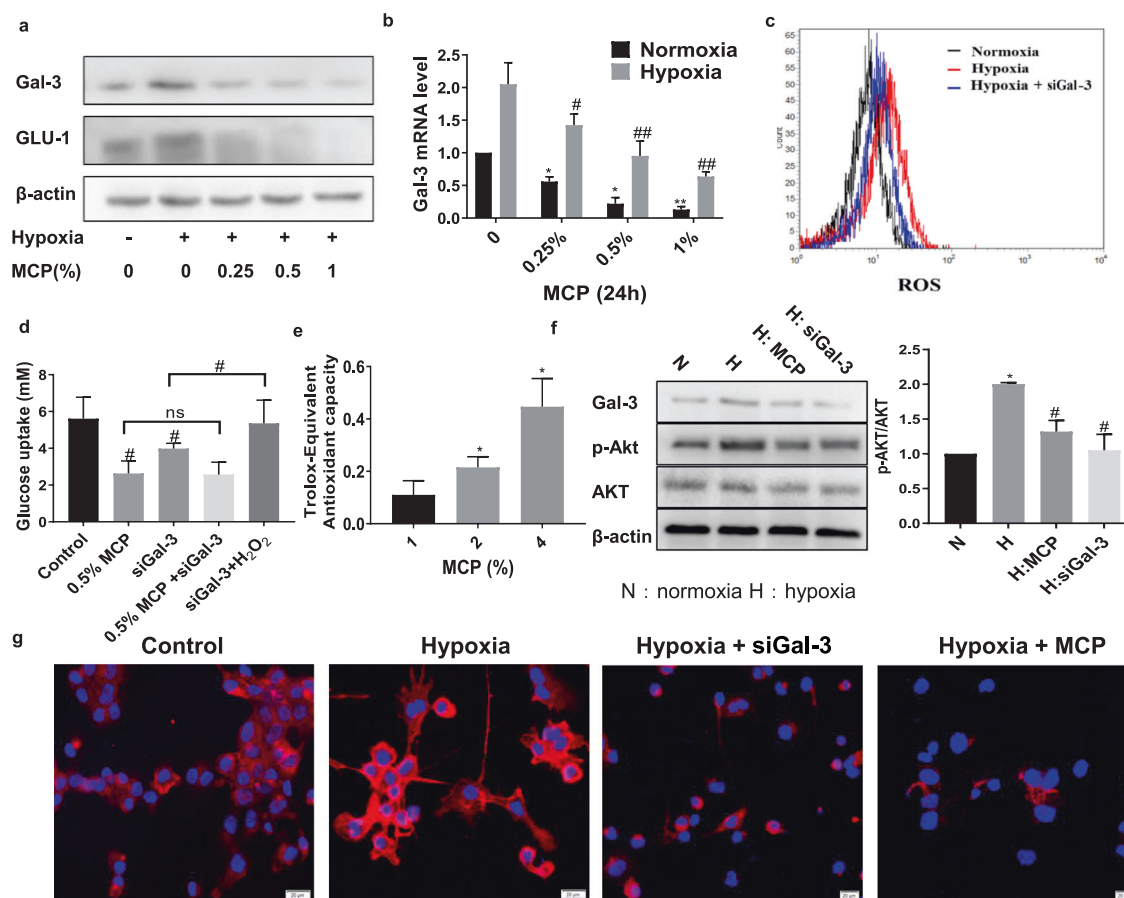


Fig. 3 MCP reduced the ROS level in TAM not only through galectin-3 inhibition, but also through its reducibility. The protein (a) and mRNA (b) expression levels of galectin-3 in TAM treated with MCP for 24 h were detected by Western blotting and RT-PCR methods. c Effect of siGal-3 on the ROS level was detected by flow cytometry method. d Effect of siGal-3 on the glucose uptake of TAM treated with MCP in hypoxia for 24 h was detected by glucose assay kit. e Redox capacity of MCP was detected by antioxidant assay. f Effects of MCP and siGal-3 on the phosphorylation of Akt in TAM were detected by Western blotting method. g Immunofluorescence images of GLUT-1 expression in hypoxia TAM treated with MCP or siGal-3 (bar = 20 μm). All the experiments have been repeated three times. **P* < 0.05, ***P* < 0.01, vs. respective normoxia control group, #*P* < 0.05, ##*P* < 0.01, vs. respective hypoxia group.

downregulated GLUT-1 expression of TAM by inhibiting ROS production and HIF-1α activity.

Considering MCP as a galectin-3 inhibitor, the role of galectin-3 in the MCP-induced inhibition of ROS level was determined. As shown in Fig. 3a, b, g, galectin-3 expression, as well as GLUT-1 expression, was significantly increased in TAM under hypoxia. The result showed that the presence of MCP inhibited the protein and mRNA expression of galectin-3 in TAM. Moreover, treatment of TAM with siGal-3 also reduced the ROS level of TAM in hypoxia which was detected by flow cytometry (Fig. 3c). After introducing H₂O₂ to TAM, the inhibition of glucose uptake by siGal-3 in hypoxic TAM was reversed (Fig. 3d). These results implied that the inhibitory effects of MCP on galectin-3 expression contributed to the decrease of ROS level and GLUT-1 expression in hypoxic TAM.

We also observed that MCP had obvious antioxidant capacity (Fig. 3e), indicating that MCP reduced the ROS level in TAM not only through galectin-3 inhibition but also through its reducibility. Besides, the presence of MCP and siGal-3 inhibited the phosphorylation of Akt, which was reported to be involved in the transport of GLUT-1 (Fig. 3f), indicating that MCP might inhibit the translocation of GLUT-1 by inhibition of galectin-3 and AKT phosphorylation.

MCP attenuated the angiogenesis-promoting and migration-promoting function of TAM on breast cancer

Human breast cancer cell MDA-MB-231 (MM231) or HUVECs were co-cultured with TAM or cultured with CM of TAM, and the effect of MCP on the TAM-mediated promotion of migration and vascular mimicry of MM231 or TAM-mediated angiogenesis of HUVECs was investigated (described as Fig. 4s). The result showed that vascular mimicry of MM231 or angiogenesis of HUVECs cultured with CM of TAM was reduced after TAM were treated with MCP (Fig. 4a). In the Transwell co-culture system, MCP attenuated the migration-promoting effect of TAM on MM231 in hypoxia (Fig. 4b). In addition, the mRNA level and secretion of VEGFA and TGF-β in hypoxic TAM were reduced by MCP (Fig. 4c, d).

MCP at noncytotoxic concentration attenuated M2-like polarization of TAM via inhibiting STAT3 phosphorylation in vitro THP-1 and TAM were treated with MCP for 24 h and cell survival was detected by CCK-8 assay. Results showed that MCP did not affect the survival of THP-1 and TAM cells at the concentration less than 0.1% (Fig. 5a, b). Then, the effect of MCP on the M2-like polarization of THP-1 was investigated. As shown in Fig. 5c, d, MCP inhibited the protein expressions of M2 surface markers CD163, CD68 and the mRNA expressions of M2 markers IL-1Rα, IL-10

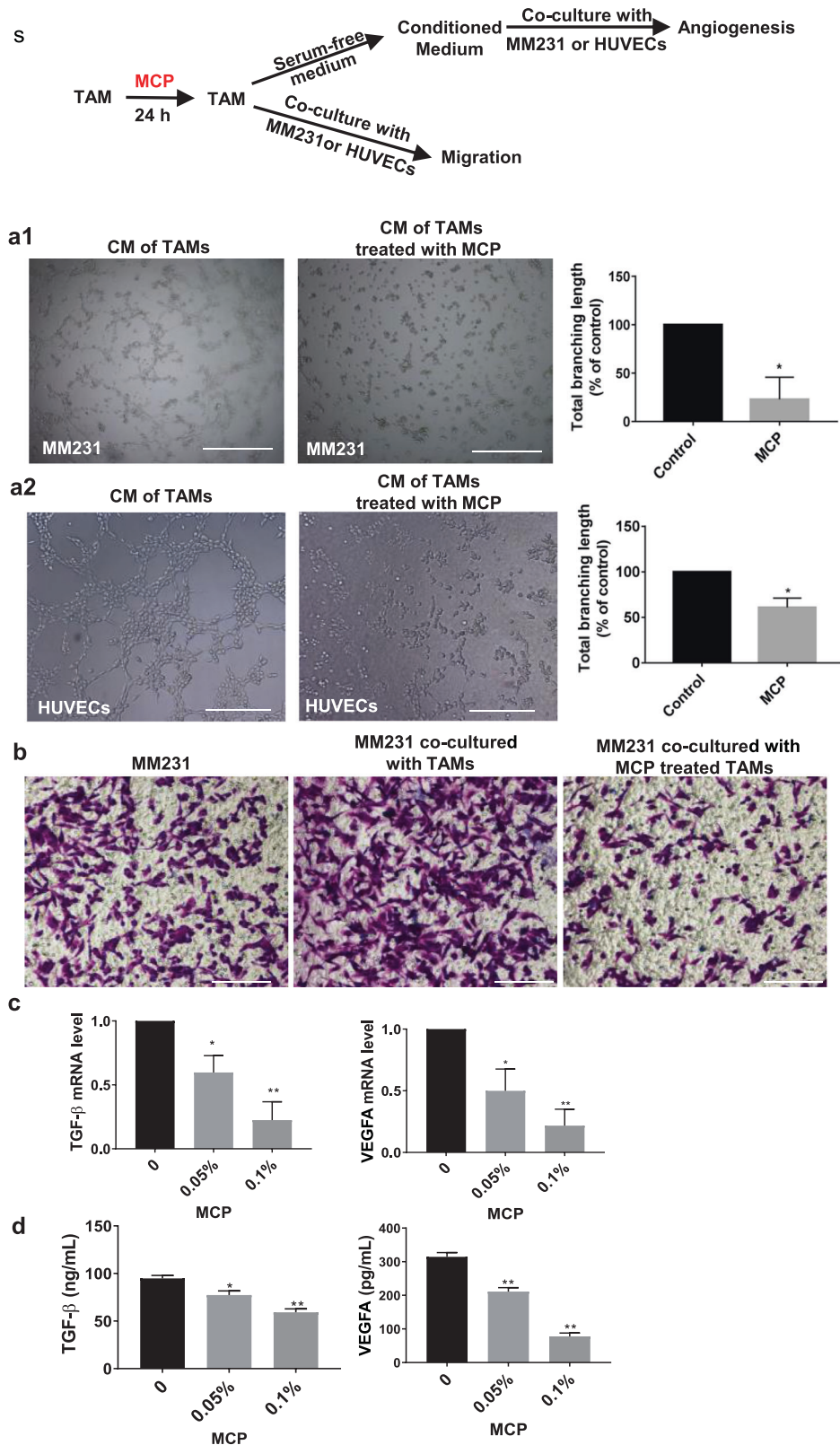


Fig. 4 MCP attenuated the tumor migration-promoting and angiogenesis-promoting function of TAM. (s) The schematic diagram of the detection of the tumor-promoting function of MCP-treated TAM. **a** Representative images of vascular mimicry of MM231 (a1) or tube formation of HUVECs (a2) by incubation with CM of TAM which was pretreated with MCP for 24 h. **b** Cell migration of MM231 in co-culture with TAM was determined by Transwell co-culture system for 24 h. **c** mRNA level of TGF- β and VEGFA in hypoxic TAM treated with MCP for 24 h were detected by RT-PCR. **d** TGF- β and VEGFA in medium supernatant of TAM treated with MCP for 24 h were determined by Western blotting method. All the experiments have been repeated three times. * $P < 0.05$, ** $P < 0.01$, vs. control group.

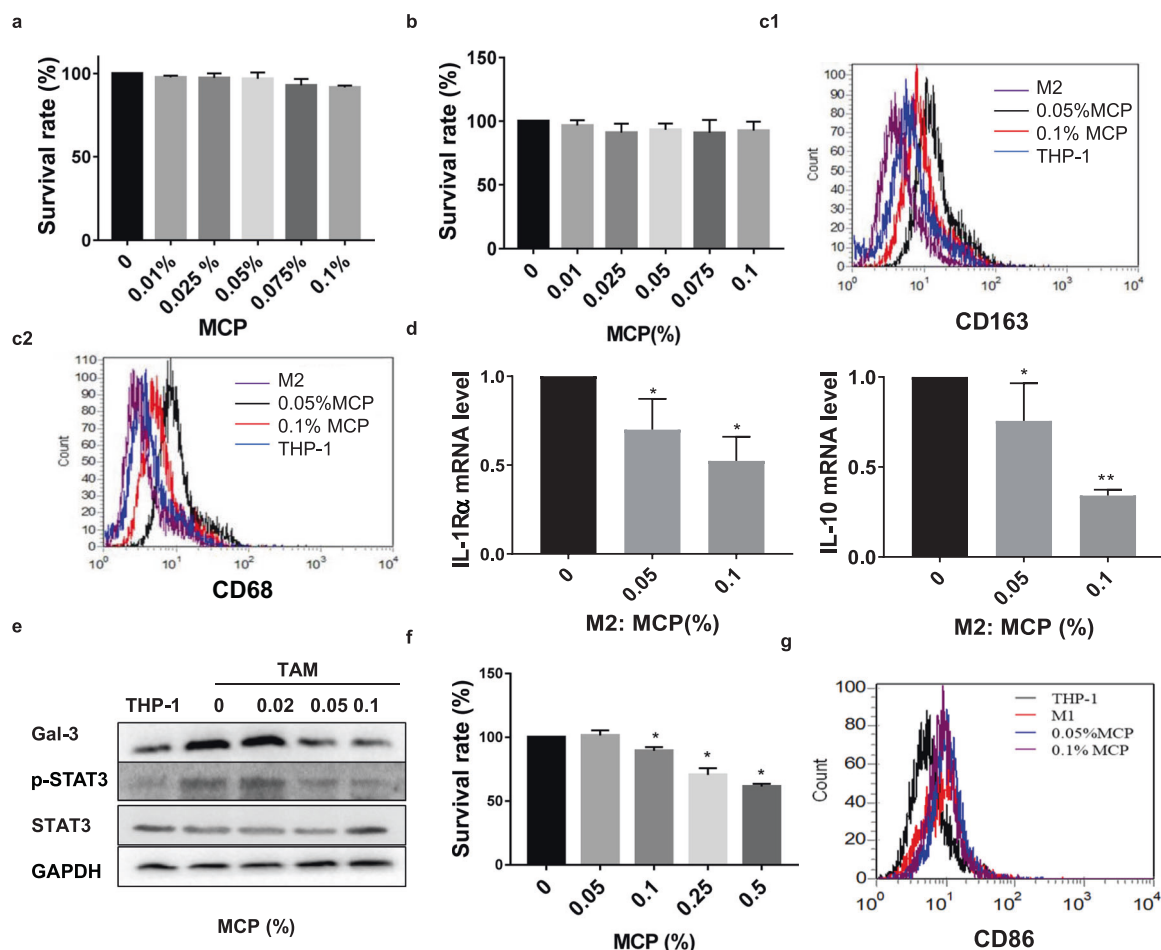


Fig. 5 MCP attenuated M2-like polarization of TAM via inhibiting STAT3 phosphorylation in vitro. **a–e** THP-1 were exposed to 20 ng/ml IL-4/IL-13 with or without MCP for 72 h. The survival rates of TAM (**a**) and THP-1 (**b**) were detected by CCK-8 assay. **c** Expressions of CD163 and CD68 in macrophages were analyzed by flow cytometry. **d** mRNA expression levels of M2 genes (IL-1R α and IL-10) were detected by RT-PCR. **e** Expressions of p-STAT3, STAT3 and galectin-3 were determined by Western blotting assay. **f–g** THP-1 were exposed to 300 IU/mL of IFN- γ and 1.0 mg/mL LPS with or without MCP for 72 h. **f** Survival rate of M1 was detected by CCK-8 assay. **g** Expression of M1 marker CD86 was analyzed by flow cytometry. All the experiments have been repeated three times. * $P < 0.05$, ** $P < 0.01$, vs. control group.

induced by IL-4/IL-13 in a concentration-dependent manner. Because STAT3 is crucially involved in the IL-4/IL-13 induced M2-like polarization, we observe the effect of MCP on the expression of STAT3 and phosphorylated STAT3 (p-STAT3) in M2-like polarization of macrophage. The result showed that IL-4/IL-13 significantly triggered the phosphorylation of STAT3 as well as the expression of galectin-3, which was significantly restrained by MCP in a dose-dependent manner (Fig. 5e), indicating that the inhibitory effects of MCP at noncytotoxic concentration on M2-like polarization of TAM was closely related to the suppression on phosphorylation of STAT3.

We further explored the effect of MCP on LPS and IFN- γ induced M1-like polarization of THP-1. The result showed that MCP had no obvious inhibitory effect on the survival of M1-like THP-1 (Fig. 5f). Meanwhile, the expression of M1 marker CD86 showed no significant change in the presence of MCP by flow cytometry (Fig. 5g), indicating that MCP did not affect the M1-like polarization of THP-1.

The tumor-promoting functions of TAM were reduced after the inhibition of M2-like polarization by 0.05% MCP. To determine the tumor-promoting function of TAM after M2-like polarization being inhibited by 0.05% MCP, the migration and vascular mimicry of MM231 or angiogenesis of HUVECs were

detected by co-culture with TAM or culture with CM of TAM (described as Fig. 6s). Results showed that vascular mimicry of MM231 or angiogenesis of HUVECs were reduced after the inhibition of TAM polarization by MCP (Fig. 6a1, a2). In the Transwell co-culture system, the migration of MM231 was increased in co-culture with M2-like polarization of TAM, however, 0.05% MCP attenuated the promotive effect of TAM on the migration of MM231 (Fig. 6b).

Besides, the proliferation, vascular mimicry and migration ability of MM231 or angiogenesis of HUVECs treated with 0.05% MCP alone were also detected. No significant effects of MCP alone was observed (Fig. 6c–e), indicating that MCP at noncytotoxic concentration could inhibit tumor progression by attenuating the M2-like polarization of TAM.

MCP inhibited breast cancer growth and metastasis by reducing M2-like polarization of TAM in vivo

The effect of MCP on tumor growth and metastasis was evaluated in 4T1-luc orthotopic breast cancer mouse model and lung metastasis model. Orthotopic tumor mice or lung metastasis model mice treated with low-dose MCP (350 mg/kg, i.g.), high-dose MCP (700 mg/kg, i.g.) and vehicle (normal saline, i.g.) for 4 or 3 weeks respectively. There was no significant difference in body weight among the three groups (Figs. 7a and 8b). The tumor

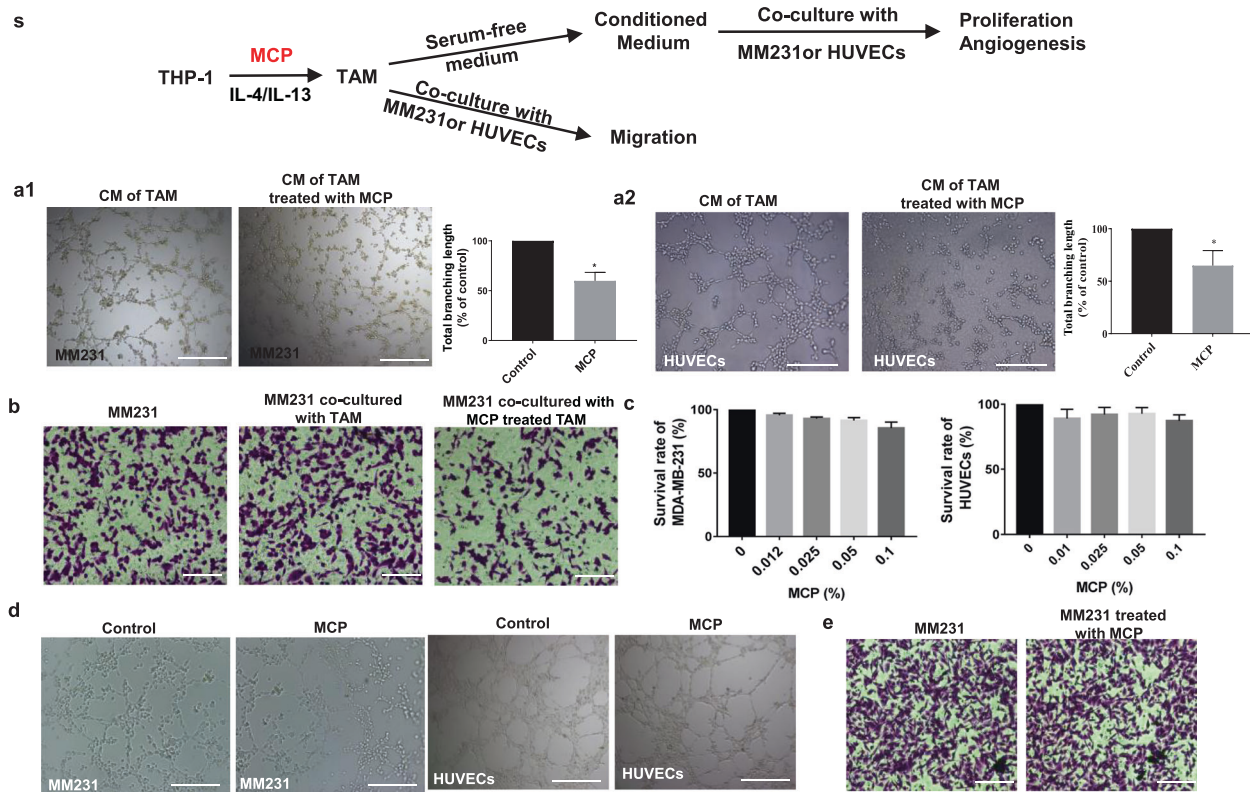


Fig. 6 The tumor-promoting function of TAM was reduced by 0.05% MCP via the inhibition of M2-like polarization. (s) The schematic diagram of detection of the tumor-promoting function of TAM after the inhibition of M2-like polarization by 0.05% MCP. **a** Representative images of vascular mimicry of MM231 (a1) or tube formation of HUVECs (a2) by incubation with CM of TAM for 6 h which was pretreated with 0.05% MCP for 72 h. **b** Cell migration of MM231 co-cultured with TAM was determined by transwell co-culture system for 24 h. **c** The proliferation of MM231 and HUVECs treated with 0.05% MCP for 24 h was assessed by CCK-8 assay. **d** Representative images of vascular mimicry of MM231 or tube formation of HUVECs treated with 0.05% MCP for 6 h. **e** Cell migration of MM231 treated with 0.05% MCP was determined by Transwell assay. All the experiments have been repeated three times. * $P < 0.05$ vs. control group.

volume in orthotopic tumor mice was significantly decreased by low-dose ($P < 0.01$) and high-dose MCP ($P < 0.05$), in comparison to that in the vehicle group (Fig. 7b). The obvious inhibitions of MCP on the orthotopic tumor growth (Fig. 7c, d) and lung metastasis (Fig. 7e) of breast cancer 4T1 cells were observed by in vivo imaging system and weighing the tumor tissues.

Treatment with MCP also significantly reduced the bioluminescence intensity and the number of pulmonary nodules of 4T1-luc cells in metastatic breast cancer model (Fig. 8a, c). These results suggested that MCP inhibited tumor pulmonary metastasis both in the orthotopic tumor model and in the metastasis model.

Furthermore, the M2-like macrophages in primary and metastatic tumors were detected by showing CD68⁺ and CD206⁺ cells using immunofluorescence technique. In comparison to the vehicle control group, MCP significantly reduced the number of CD68⁺ and CD206⁺ cells in tumors, indicating that MCP suppressed M2-like macrophages (Figs. 7f and 8d). In addition, MCP obviously inhibited tumor angiogenesis as indicated by reduced CD31 expression in tumor tissues (Fig. 7h). Consistent with the data in vitro, the lactate acid level in tumor tissue was also decreased by MCP (Fig. 7g).

To determine the inhibitory effect of MCP on the tumor metastasis via targeting macrophages, clodronate liposomes (CL) was introduced to deplete macrophages in the mouse. The results showed that administration of CL (100 μ L/20 g every week) could inhibit tumor growth and metastasis in orthotopic tumor mice model (Fig. 7j, k, i, m), as well as lung metastasis in metastatic tumor mice model (Fig. 8e). Compared with single CL treatment, the combination of MCP (700 mg/kg) with CL did not significantly increase the anti-tumor effect. This suggested that MCP could inhibit tumor development via targeting TAM.

DISCUSSION

In search of natural substances that could be used to treat cancer, MCP, as dietary fibers, have been reported to possess inhibitory effects on the development of colon cancer, prostate cancer, melanoma, multiple myeloma, breast cancer and angiosarcoma [7, 13–17]. In the present study, it is the first time to investigate the effect of MCP on the survival and polarization of TAM in the hypoxia microenvironment.

Firstly, we found that MCP suppressed the survival of TAM with a higher inhibitory effect in hypoxia than in normoxia. This indicated that MCP exhibited promising cytotoxicity toward hypoxic macrophages. Hypoxia is an important feature of the tumor microenvironment. TAM accumulates at high density in hypoxic areas of tumors and responds to hypoxia by secreting cytokines that promote tumor cell proliferation, invasion and metastasis, and tumor angiogenesis [18, 19]. However, several studies have shown that TAM in the area near tumor blood vessels with sufficient oxygen supply may play a beneficial role because TAM in these areas is associated with a favorable prognosis [1, 20]. Therefore, targeting TAM in the hypoxia region without affecting TAM in the normoxia region would be a potential therapeutic strategy.

It was found in this study that MCP inhibited the increased glucose uptake of TAM induced by hypoxia via downregulation of GLUT-1 expression, and consequently reducing the viability of TAM in hypoxia environment. GLUT-1, a major protein mediating cellular glucose uptake, is an attractive therapeutic target in cancer treatment. Under hypoxia and other abnormal conditions, the expression of GLUT-1 is upregulated, resulting in an increased dependence on anaerobic glycolysis as an energy source [21]. It has been reported that the expression of galectin-3 and GLUT-1

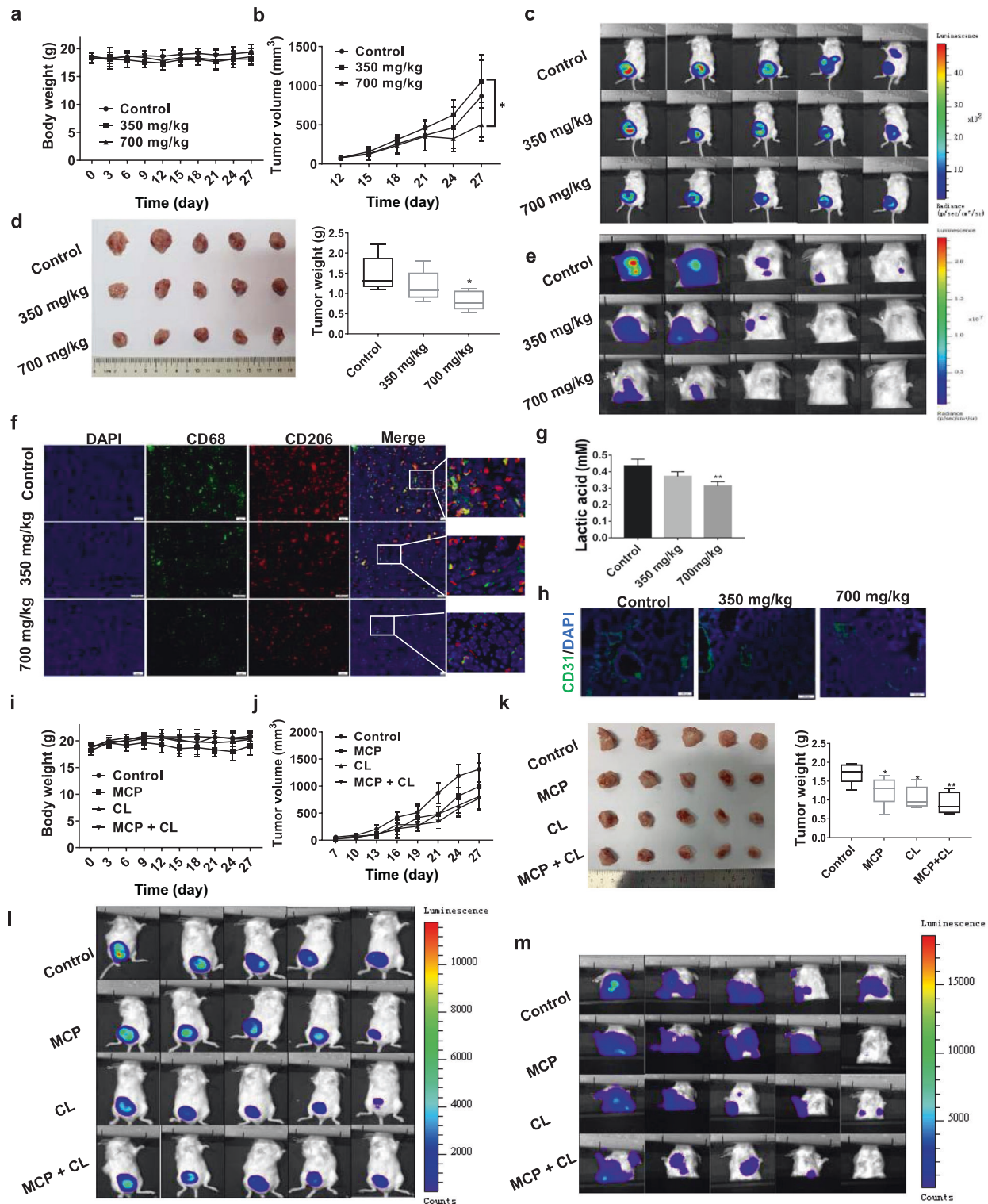


Fig. 7 MCP inhibited tumor growth and lung metastasis in breast cancer 4T1-luc orthotopic transplantation model by targeting M2-like polarization of TAM. **a, b, i, j** The body weight and tumor volume of mice were recorded during the animal experiment. **c, e, l, m** The growth and lung metastasis of breast cancer were observed using an in vivo imaging system. **d, k** At the end of the experiment, mice were sacrificed and the tumor tissue was weighed. **f, h** CD68, CD206 positive and CD31 positive cells in tumors were detected by immunofluorescence using antibody against FITC- CD68, PE-CD206 and CD31, respectively. **g** The lactate acid level in tumor tissue was detected by lactate acid assay. All data are presented as means \pm SD, $n = 5$, * $P < 0.05$, ** $P < 0.01$ vs. control group.

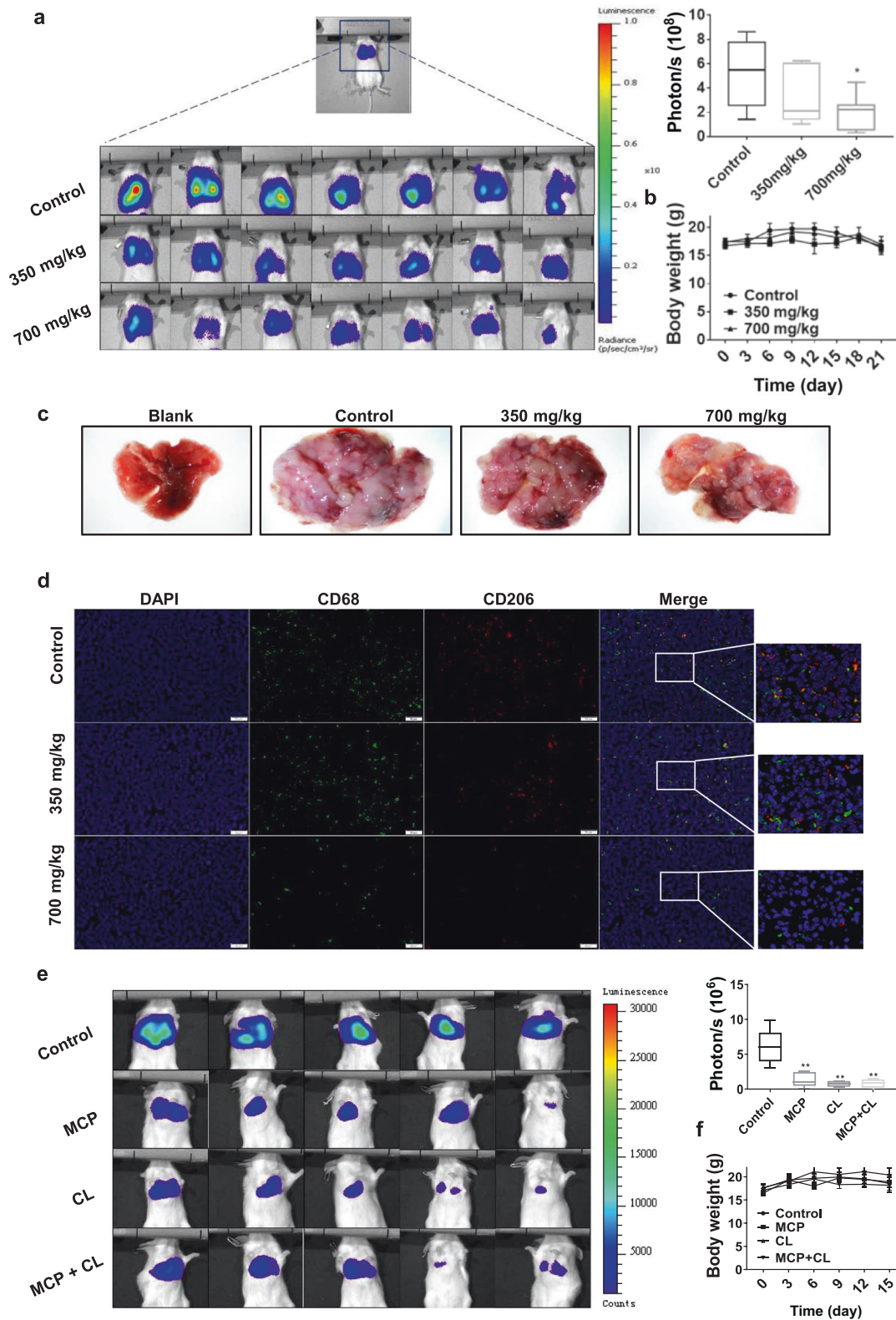


Fig. 8 MCP inhibited lung metastasis of breast cancer in intravenous model by reducing M2-like polarization of TAM. **a, e** The lung metastasis was observed using an in vivo imaging system. **b, f** The body weight of mice was recorded every 3 days for 21 days or 15 days. **c** Representative lung tissue in each group. **d** CD68 and CD206 positive cells in lung tissue were detected by immunofluorescence using FITC-CD68 and PE-CD206 antibody. All data are presented as means \pm SD, $n = 7$, $*P < 0.05$, $**P < 0.01$ vs. control group.

increased in colorectal adenocarcinoma and correlated with poor prognosis [22], suggesting that galectin-3 might have a certain relation with GLUT-1. MCP has been shown a cytotoxic effect on tumor cells through binding to the carbohydrate recognition domain of galectin-3 to inhibit its function [23]. In this study, the upregulation of galectin-3 in TAM under hypoxia was consistent with the previous report that galectin-3 was upregulated under hypoxia in different cell types [24, 25]. And the suppression of galectin-3 in TAM by MCP or siRNA could both inhibit hypoxia-mediated GLUT-1 expression, indicating that galectin-3 may be involved in the downregulation of GLUT-1 expression induced by MCP.

The generation of ROS has been shown to be crucially involved in the regulation of glucose transport (GLUT-mediated), which is frequently upregulated by hypoxia [26]. ROS can affect the translocation of GLUT-1 and the expression of GLUT-1 through GLUT-1 transcription factor HIF-1 α [27, 28]. In this study, we found that MCP reduced ROS through inhibiting galectin-3, thus inhibiting HIF-1 α and GLUT-1 expression. Besides, MCP can also directly reduce ROS level in TAM by its reducibility. The relationship between ROS and galectin-3 is complicated. One study showed that galectin-3 knockout animals presented lower ROS production [29]. However, Matarrese et al. reported that in human breast cancer cell line, galectin-3 overexpression reduced ROS generation [30]. Our results showed that either siGal-3 or MCP treatment reduces ROS in hypoxic TAM. These suggest that the regulatory effect of galectin-3 on ROS depends on cell types and different conditions. And as it was reported that the ROS level decreased after inhibition of glycolysis [31], the GLUT-1 reduced by the downregulation of ROS leads to inhibition of glycolysis, in turn reducing ROS levels. Therefore, there might exist a feedback loop between ROS and GLUT-1 in TAM with MCP treatment.

TAM are classified into M1 and M2 phenotypes, which translates to tumor suppressive (M1) or tumor supportive (M2) [20]. Thus, inhibiting M2 like polarization of macrophages has been found to be an effective anti-tumor strategy [32]. STAT3 is known to serve the regulation of M2-like macrophage phenotype as a downstream protein of IL-4R signaling [20]. Studies have documented the effect of galectin-3 or MCP on the STAT3 phosphorylation in endothelial cells, microglia and astrocytes [33, 34]. And it was reported that galectin-3 was involved in the polarization of macrophage [35, 36]. In this study, we found that MCP, as galectin-3 inhibitor, inhibited M2 polarization by downregulating STAT3 phosphorylation. In the next study, we will further elucidate the role and molecular mechanism of galectin-3 in the inhibition of M2 polarization induced by MCP.

We also observed that noncytotoxic concentration of MCP on macrophages did not inhibit the migration and angiogenesis of breast cancer cells or HUVECs, however, it could inhibit the tumor migration-promoting and angiogenesis-promoting functions of M2-like TAM in hypoxia, which indicated that MCP at lower concentration could inhibit the migration and angiogenesis of tumor cells by interfering with M2 polarization of macrophages.

We further investigated the effect of MCP on the tumor-promoting function of TAM in mice tumor models. Results showed that MCP significantly inhibited tumor orthotopic growth and pulmonary metastases. To evaluate whether MCP affects circulating tumor cell seeding at metastatic sites, tumor lung metastasis mice models was also established. Results also showed that MCP inhibited pulmonary metastasis of breast cancer cells. In addition, MCP not only decreased the percentage of M2-like TAM in primary tumor tissues but also suppressed M2-like TAM at metastatic sites. Moreover, MCP decreased the angiogenesis of breast cancer cells by detecting CD31 expression in tumor tissues. These suggest that MCP prevents lung metastasis of breast cancer by inhibiting angiogenesis through targeting M2 macrophages.

In conclusion, MCP suppressed TAM survival and M2-like polarization *in vitro* and *in vivo*. As a natural dietary fiber, MCP alone or in combination with other therapeutic strategies, especially the antiangiogenic strategy which can promote TAM infiltration [37], may be a potential therapeutic strategy for cancer treatment and deserves further investigations.

ACKNOWLEDGEMENTS

This work was supported by the Natural Science Foundation of Shandong Province [ZR2020MH419], National Natural Science Foundation of China Grants [82173843], Key Research and Development Program of Shandong Province [2017CXGC1401], and China-Australia Centre for Health Sciences Research [CACHSR no. 2019GJ01].

AUTHOR CONTRIBUTIONS

XLG was responsible for designing the experiments, research supervision, and drafting the manuscript. LW was responsible for conducting most of the experiments and drafting the manuscript. LZ, DDD, and CS were responsible for performing part of the experiment and analyzing data. FLG and XXY were responsible for drafting the manuscript. All authors read and approved the final manuscript.

ADDITIONAL INFORMATION

Competing interests: The authors declare no competing interests.

REFERENCES

1. Yang M, McKay D, Pollard JW, Lewis CE. Diverse functions of macrophages in different tumor microenvironments. *Cancer Res.* 2018;78:5492–503.
2. Cannarile MA, Weisser M, Jacob W, Jegg AM, Ries CH, Rüttinger D. Colony-stimulating factor 1 receptor (CSF1R) inhibitors in cancer therapy. *J Immunother Cancer.* 2017;5:53.
3. Henderson NC, Sethi T. The regulation of inflammation by galectin-3. *Immunol Rev.* 2009;230:160–71.
4. Harrison SA, Marri SR, Chalasani N, Kohli R, Aronstein W, Thompson GA, et al. Randomised clinical study: GR-MD-02, a galectin-3 inhibitor, vs. placebo in patients having non-alcoholic steatohepatitis with advanced fibrosis. *Aliment Pharmacol Ther.* 2016;44:1183–98.
5. Mirandola L, Yu YF, Chui K, Jenkins MR, Cobos E, John CM, et al. Galectin-3C inhibits tumor growth and increases the anticancer activity of bortezomib in a murine model of human multiple myeloma. *PLoS One.* 2011;6:e21811.
6. Hossein G, Halvaei S, Heidarian Y, Dehghani-Ghobadi Z, Hassani M, Hosseini H, et al. Pectasol-C modified citrus pectin targets galectin-3-induced STAT3 activation and synergize paclitaxel cytotoxic effect on ovarian cancer spheroids. *Cancer Med.* 2019;8:4315–29.
7. Glinsky VV, Raz A. Modified citrus pectin anti-metastatic properties: one bullet, multiple targets. *Carbohydr Res.* 2009;344:1788–91.
8. Liu HY, Huang ZJ, Yang GH, Lu WQ, Yu NR. Inhibitory effect of modified citrus pectin on liver metastases in a mouse colon cancer model. *World J Gastroenterol.* 2008;14:7386–91.
9. Nangia-Makker P, Hogan V, Honjo Y, Baccarini S, Tait L, Bresalier R, et al. Inhibition of human cancer cell growth and metastasis in nude mice by oral intake of modified citrus pectin. *J Natl Cancer Inst.* 2002;94:1854–62.
10. Wang L, Li YS, Yu LG, Zhang XK, Zhao L, Gong FL, et al. Galectin-3 expression and secretion by tumor-associated macrophages in hypoxia promotes breast cancer progression. *Biochem Pharmacol.* 2020;178:114113.
11. Winstel V, Schneewind O, Missiakas D. *Staphylococcus aureus* exploits the host apoptotic pathway to persist during infection. *mBio* 2019;10:e02270–19.
12. Paik JY, Jung KH, Lee JH, Park JW, Lee KH. Reactive oxygen species-driven HIF1 α triggers accelerated glycolysis in endothelial cells exposed to low oxygen tension. *Nucl Med Biol.* 2017;45:8–14.
13. Jiang J, Eliaz I, Sliva D. Synergistic and additive effects of modified citrus pectin with two polybotanical compounds, in the suppression of invasive behavior of human breast and prostate cancer cells. *Integr Cancer Ther.* 2013; 12:145–52.
14. Kolatsi-Joannou M, Price KL, Winyard PJ, Long DA. Modified citrus pectin reduces galectin-3 expression and disease severity in experimental acute kidney injury. *PLoS One.* 2011;6:e18683.
15. Yan J, Katz A. PectaSol-C modified citrus pectin induces apoptosis and inhibition of proliferation in human and mouse androgen-dependent and -independent prostate cancer cells. *Integr Cancer Ther.* 2010;9:197–203.

16. Fang T, Liu DD, Ning HM, Dan Liu, Sun JY, Huang XJ, et al. Modified citrus pectin inhibited bladder tumor growth through downregulation of galectin-3. *Acta Pharmacol Sin.* 2018;39:1885–93.
17. Zhao ZY, Liang L, Fan X, Yu Z, Hotchkiss AT, Wilk BJ, et al. The role of modified citrus pectin as an effective chelator of lead in children hospitalized with toxic lead levels. *Alter Ther Health Med.* 2008;14:34–8.
18. Lewis C, Murdoch C. Macrophage responses to hypoxia: implications for tumor progression and anti-cancer therapies. *Am J Pathol.* 2005;167:627–35.
19. Locati M, Curtale G, Mantovani A. Diversity, mechanisms, and significance of macrophage plasticity. *Annu Rev Pathol.* 2020;15:123–47.
20. Tamura R, Tanaka T, Yamamoto Y, Akasaki Y, Sasaki H. Dual role of macrophage in tumor immunity. *Immunotherapy* 2018;10:899–909.
21. Iwasaki K, Yabushita H, Ueno T, Wakatsuki A. Role of hypoxia-inducible factor-1 α , carbonic anhydrase-IX, glucose transporter-1 and vascular endothelial growth factor associated with lymph node metastasis and recurrence in patients with locally advanced cervical cancer. *Oncol Lett.* 2015;10:1970–8.
22. Rashed HE, Ahmed SA, Abdelgawad M. Clinicopathologic significance of galectin-3 and glucose transporter 1 expressions in colorectal cancer. *Life Sci J* 2015;12:9–11.
23. Menachem A, Bodner O, Pastor J, Raz A, Kloog Y. Inhibition of malignant thyroid carcinoma cell proliferation by Ras and galectin-3 inhibitors. *Cell Death Discov.* 2015;1:15047.
24. de Oliveira JT, Ribeiro C, Barros R, Gomes C, de Matos AJ, Reis CA, et al. Hypoxia up-regulates galectin-3 in mammary tumor progression and metastasis. *PLoS One.* 2015;10:e0134458.
25. Zheng J, Lu W, Wang C, Xing Y, Chen X, Ai Z. Galectin-3 induced by hypoxia promotes cell migration in thyroid cancer cells. *Oncotarget.* 2017;8:101475–88.
26. Prata C, Maraldi T, Fiorentini D, Zambonin L, Hakim G, Landi L. Nox-generated ROS modulate glucose uptake in a leukaemic cell line. *Free Radic Res.* 2008;42:405–14.
27. Fiorentini D, Prata C, Maraldi T, Zambonin L, Bonsi L, Hakim G, et al. Contribution of reactive oxygen species to the regulation of Glut1 in two hemopoietic cell lines differing in cytokine sensitivity. *Free Radic Biol Med.* 2004;37:1402–11.
28. Ryu JM, Lee HJ, Jung YH, Lee KH, Kim DI, Kim JY, et al. Regulation of stem cell fate by ROS-mediated alteration of metabolism. *Int J Stem Cells.* 2015;8:24–35.
29. Fernandes Bertocchi AP, Campanhole G, Wang PHM, Gonçalves GM, Damião MJ, Cenedeze MA. A role for galectin-3 in renal tissue damage triggered by ischemia and reperfusion injury. *Transpl Int.* 2008;21:999–1007.
30. Matarrese P, Tinari N, Semeraro ML, Natoli C, Iacobelli S, Malorni W. Galectin-3 overexpression protects from cell damage and death by influencing mitochondrial homeostasis. *FEBS Lett.* 2000;473:311–5.
31. Wang Q, Zhao Y, Sun M, Liu S, Li B, Zhang L, et al. 2-Deoxy-d-glucose attenuates sevoflurane-induced neuroinflammation through nuclear factor-kappa B pathway in vitro. *Toxicol Vitr.* 2014;28:1183–9.
32. Mantovani A, Marchesi F, Malesci A, Laghi L, Allavena P. Tumour-associated macrophages as treatment targets in oncology. *Nat Rev Clin Oncol.* 2017;14:399–416.
33. Nishikawa H, Suzuki H. Response by Nishikawa and Suzuki to Letter Regarding Article, “Modified citrus pectin prevents blood-brain barrier disruption in mouse subarachnoid hemorrhage by inhibiting galectin-3”. *Stroke.* 2019;50:e137.
34. Jeon SB, Yoon HJ, Chang CY, Koh HS, Jeon SH, Park EJ. Galectin-3 exerts cytokine-like regulatory actions through the JAK-STAT pathway. *J Immunol.* 2010;185:7037–46.
35. Mackinnon AC, Farnworth SL, Hodgkinson PS, Henderson NC, Atkinson KM, Leffler H, et al. Regulation of alternative macrophage activation by galectin-3. *J Immunol.* 2008;180:2650–8.
36. Dong S, Hughes RC. Macrophage surface glycoproteins binding to galectin-3 (Mac-2-antigen). *Glycoconj J.* 1997;14:267–74.
37. Zhang W, Zhu XD, Sun HC, Xiong YQ, Zhuang PY, Xu HX, et al. Depletion of tumor-associated macrophages enhances the effect of sorafenib in metastatic liver cancer models by antimetastatic and antiangiogenic effects. *Clin Cancer Res.* 2010;16:3420–30.